

Application of DTA-TG-MS for determination of chemical stability of BaCeO_{3-δ}-based protonic conductors

Paweł Pasierb · Ryszard Gajerski ·
Magdalena Osiadły · Agnieszka Łącz

Received: 11 October 2013 / Accepted: 8 March 2014 / Published online: 13 April 2014
© The Author(s) 2014. This article is published with open access at Springerlink.com

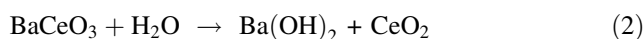
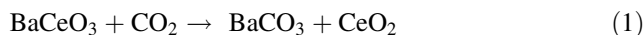
Abstract Thermogravimetry (TG) and Differential Thermal Analysis (DTA) techniques coupled with mass spectrometry were applied to evaluate the chemical stability of BaCeO_{3-δ}-based materials in the CO₂- and H₂O-rich atmosphere. The different groups of materials were investigated: solid solutions of BaCeO₃-BaTiO₃ and BaCeO₃-BaSnO₃ acceptor doped by Y or In and composite materials with nominal composition (1-x)BaCe_{0.9}Y_{0.1}O_{3-δ}-xYPO₄. To evaluate the chemical stability towards carbon dioxide and water vapour samples were exposed to atmosphere containing CO₂/H₂O (7 % of CO₂ in air, 100 % RH) at temperature of 25 °C for 350 h. Thermal analysis (TG/DTA) was applied to analyse the materials before and after the test. To support the interpretation of TG/DTA results, the analysis of gaseous products evolved during thermal treatment of the samples was provided using mass spectrometer. This combined analysis clearly shows that during the exposition test, the conversion of barium cerate to barium carbonate and barium hydroxide occurs. The amount of BaCO₃ and the degree of BaCeO_{3-δ} conversion depend on the type of barium cerate modification. The mass loss observed after the exposition test can be treated as a measure of chemical instability of BaCeO_{3-δ}-based materials. The correlation of chemical stability, described by the mass loss, on Goldschmidt tolerance factor, describing the deviation from ideal perovskite structure, was found in most of the materials investigated. However, the influence of the microstructure and the

modification the grain boundaries on the chemical stability of BaCeO_{3-δ}-based materials cannot be neglected.

Keywords DTA · TG · Protonic conductors · Barium cerate · Barium cerium oxide · Barium phosphate · Composites · Chemical stability

Introduction

One of the greatest disadvantages of proton conductors based on BaCeO_{3-δ} is poor chemical stability especially in atmospheres containing CO₂ and H₂O. Despite the high-protonic conductivity, unacceptably low-chemical stability resulting in decreasing the mechanical durability limits possible applications of these materials. The reason of poor chemical stability of BaCeO_{3-δ}-based materials is possibility of barium cerate reaction with CO₂ and H₂O resulting the formation of secondary BaCO₃ (or Ba(OH)₂) and cerium oxide according to the reactions [1, 2]

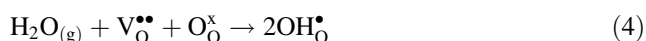


The chemical stability of BaCeO_{3-δ}-based materials can be discussed, depending on the temperature range, on the level of working (generally 400–800 °C) or storage (room temperature) conditions. Studies presented in the literature are mainly focused on high-temperature corrosion which occurs where materials are used. In order to verify the stability towards CO₂, samples are exposed to CO₂-containing atmosphere in the relatively high-temperature (600–800 °C) for a long period of time (up to 200 h) [3–9], which simulates the working conditions of electrochemical devices built from these materials. The XRD analysis of

P. Pasierb (✉) · R. Gajerski · M. Osiadły · A. Łącz
AGH University of Science and Technology, Faculty of
Materials Science and Ceramics, al. A Mickiewicza 30,
30-059 Kraków, Poland
e-mail: ppasierb@agh.edu.pl

materials after such tests clearly shows the presence of barium carbonate which indicates that during the exposition of $\text{BaCeO}_{3-\delta}$ -based materials to the CO_2 -rich atmospheres the reaction (1) occurs. To evaluate the stability of $\text{BaCeO}_{3-\delta}$ -based materials towards CO_2 , the thermogravimetry (TG) can be also applied. Increase of the mass observed during heating of the samples in the carbon dioxide atmosphere corresponds to CO_2 absorption which leads to production of the secondary barium carbonate [1, 4]. On the other hand, the mass loss observed while the samples after the exposition on CO_2 are heated is connected with the decomposition of secondary barium carbonate formed [1]. To evaluate the stability of $\text{BaCeO}_{3-\delta}$ -based materials towards H_2O , boiling the samples in the water is usually performed [4, 5, 10]. The presence of $\text{Ba}(\text{OH})_2$ in the samples after the test is the confirmation that during the test, the reaction (2) takes place. Thus, the amount of BaCO_3 or $\text{Ba}(\text{OH})_2$ in the samples after the tests can be treated as the measure of chemical instability of $\text{BaCeO}_{3-\delta}$ -based materials towards CO_2 - or H_2O -containing atmospheres.

The modifications of materials based on perovskite-type structure of $\text{BaCeO}_{3-\delta}$ are focused on increasing the chemical stability with maintaining relatively high-ionic conductivity. These modifications are usually based on introduction of acceptor dopant M^{3+} (like Y^{3+} , In^{3+} , Yb^{3+} or Nd^{3+}) into the barium cerate [11–16], which indirectly leads to the increase of the concentration of protonic defects in the water-/hydrogen-rich atmosphere according to the reactions



Unfortunately, in most cases, the decrease of chemical stability is observed for materials modified by acceptor doping.

Based on thermodynamic data, it can be stated that BaTiO_3 , BaZrO_3 or BaSnO_3 exhibit much higher chemical stability towards CO_2 than barium cerate. The incorporation of zirconium or titanium into the $\text{BaCeO}_{3-\delta}$ lattice and formation of solid solutions $\text{BaCe}_{1-x}\text{M}_x\text{O}_{3-\delta}$ ($\text{M} = \text{Zr}, \text{Ti}$) seem to be the natural way to enhance chemical stability [1, 17–19]. In such cases, the decrease of electrical conductivity is observed. Currently, the optimal compositions were recognized, where the amounts of both types of dopants are the compromise between the stability and the electrical conductivity. Commonly, the $\text{BaCe}_{0.7}\text{Zr}_{0.2}\text{Y}_{0.1}\text{O}_{3-\delta}$ is considered to be the best material for construction of different electrochemical devices [1]. Some experiments showed that $\text{BaCe}_{0.7}\text{Zr}_{0.2}\text{Y}_{0.1}\text{O}_{3-\delta}$ may still have unsatisfactory stability, and the latest $\text{BaCeO}_{3-\delta}$ -based materials proceed to zirconium richer compositions [20].

The influence of dopants used on chemical stability can be discussed taking into account the modification of crystallographic structure, where the ionic radius of host and dopant atoms are the crucial parameters. The detailed discussion using the Goldschmidt tolerance factor, which describes the departure from ideal cubic structure, and its dependence on the ionic radius of dopants used will be presented in Results part.

In this work, the dopants used were selected based on the dependence of chemical stability on the structure. An yttrium and indium were chosen as the acceptor dopants as the ionic radii of Ce^{4+} (0.087 nm) is slightly smaller than for Y^{3+} (0.090 nm) and slightly greater than for In^{3+} (0.080 nm) [21]. Titanium and tin were used as possible alternative to Zr dopant, which was widely described in the literature. Additionally, we have tested composite materials which is the completely different approach towards improved stability and electrical conductivity. The properties of composite materials with nominal composition of $(1-x)\text{BaCe}(\text{Y})\text{O}_{3-\delta} - x\text{YPO}_4$ ($x = 0.05\text{--}0.2$) system were tested and compared with the single-phase-doped materials.

The main purpose of this work was to evaluate the functionality of the DTA-TG-MS method for determination of chemical stability of $\text{BaCeO}_{3-\delta}$ -based protonic conductors towards CO_2 and H_2O vapours. In this work, the materials after low-temperature corrosion tests (simulating storage conditions) were measured in order to complement the literature data concerning materials mostly after high-temperature corrosion tests which correspond to working conditions of materials.

Experimental and sample preparation

Four groups of materials were synthesized:

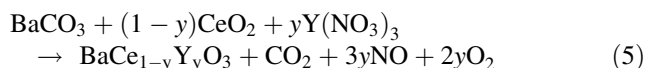
- solid solutions of $\text{BaCeO}_3\text{--BaTiO}_3$ and $\text{BaCeO}_3\text{--BaSnO}_3$ with nominal composition: $\text{BaCe}_{1-x}\text{Ti}_x\text{O}_{3-\delta}$ ($x = 0.05\text{--}0.3$) and $\text{BaCe}_{1-x}\text{Sn}_x\text{O}_{3-\delta}$ ($x = 0.01\text{--}0.2$)
- solid solutions of $\text{BaCeO}_3\text{--BaTiO}_3$ and $\text{BaCeO}_3\text{--BaSnO}_3$ with acceptor dopants, nominal composition: $\text{Ba}(\text{Ce}_{1-x}\text{Sn}_x)\text{In}_y\text{O}_{3-\delta}$ ($x = 0.05$, $y = 0.01\text{--}0.2$) and $\text{Ba}(\text{Ce}_{1-x}\text{Ti}_x)\text{Y}_y\text{O}_{3-\delta}$ ($x = 0.05$, $y = 0.05\text{--}0.2$).
- composite materials with nominal composition $(1-x)\text{BaCe}_{0.9}\text{Y}_{0.1}\text{O}_{3-\delta} - x\text{YPO}_4$ ($x = 0.05\text{--}0.2$)
- $\text{BaCeO}_{3-\delta}$ and $\text{BaCe}_{0.9}\text{Y}_{0.1}\text{O}_{3-\delta}$ as a reference samples.

All materials were prepared by solid state reaction method. The required amounts of high-purity substrates, supplied by Aldrich Chemical Company Inc.: barium carbonate BaCO_3 (99 + % A.C.S. reagent), cerium(IV) oxide CeO_2 (99.9 %), diammonium hydrogen phosphate $(\text{NH}_4)_2\text{HPO}_4$ (98 + % A.C.S. reagent), anatase TiO_2 (99.7 %) and

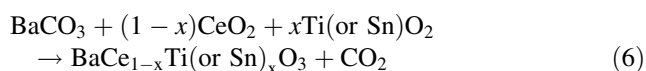
tin(IV) oxide SnO_2 (99.9 %) powders, $\text{Y}(\text{NO}_3)_3 \cdot 6\text{H}_2\text{O}$ (99.8 %) and $\text{In}(\text{NO}_3)_3 \cdot x\text{H}_2\text{O}$ (99.9 %) (used as water solutions with concentrations 0.28 and 0.15 M, respectively), were used to prepare the materials. After mixing the starting powders and the impregnation by solution of yttrium or indium nitrate, the materials were dried at 80 °C for 12 h and then crushed in the agate mortar. Obtained powders were formed in the pallet die and calcinated at 1,200 °C for 24 h. The detailed parameters of calcinations were established based on TG/DTA results (SDT 2960 TA Instruments, mass about 50 mg, heating rate 10 °C min^{-1} , synthetic air atmosphere, platinum crucibles) supported by mass spectrometry MS analysis of the gaseous products (QMD 300 ThermoStar Balzers) and by XRD analysis (Philips X'Pert with $\text{CuK}\alpha$ radiation) of obtained products. Received materials were crushed and milled in the absolute alcohol suspension with ZrO_2 -grinding media ($\phi = 5$ mm, suppl.: Tosoh, Japan). After drying powders were formed in a pellet die, isostatically pressed (250 MPa) and sintered at 1,600 °C for 3 h in air atmosphere. All obtained materials were stored in desiccator to avoid any secondary reactions, especially with CO_2 and H_2O vapours.

Based on TG/DTA measurements, MS and XRD results, the general reactions of formation of $\text{BaCeO}_{3-\delta}$ -based materials can be described according to chemical reactions given below.

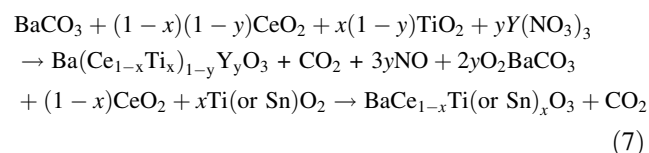
In the case of yttrium-dope



The formation of solid solution of barium cerium–titanium oxide and barium cerium–tin oxide

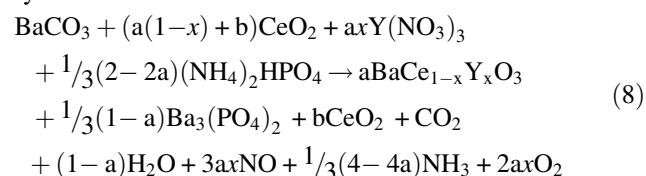


The formation of yttrium-doped barium cerium–titanium oxide



The reaction of indium-doped barium cerium–tin oxide ($\text{Ba}(\text{Ce}_{1-x}\text{Sn}_x)_{1-y}\text{In}_y\text{O}_{3-\delta}$) formation can be written analogically to Eq. (7).

The synthesis of composite materials can be simplified by the reaction:



where a and b correspond to the amount of $\text{Ba}_3(\text{PO}_4)_2$ and CeO_2 phases formed.

Equations (5–8) written above do not describe the mechanism of the reactions but only follow the stoichiometry and the phase composition of obtained materials, according to the XRD data, as discussed below.

Thermogravimetry, differential thermal analysis (DTA) and mass spectrometry (MS) were applied for evaluation of stability of $\text{BaCeO}_{3-\delta}$ -based materials in the presence of CO_2 and H_2O . All samples were exposed to the atmosphere containing CO_2 and H_2O (7 % of CO_2 in air, 100 % RH) at 25 °C for two weeks (about 350 h). After this exposition, test samples of mass about 50 mg were heated in the platinum crucible with the rate of 10 deg min^{-1} in synthetic air atmosphere with flow rate 6 $\text{dm}^3 \text{h}^{-1}$. The quadruple mass spectrometer QMD 300 ThermoStar (Balzers) operated with an electron impact ionizer (70 eV) connected on-line with SDT apparatus by the heated (up to 200 °C) quartz capillary was applied to support the interpretation of the thermal decomposition results of the samples before and after the exposition test. The amount of CO_2 evolved during this measurement and the mass loss were treated directly in this comparative test as a measure of the chemical instability of the materials tested.

To determine the phase composition and crystallographic structure of obtained materials, X-ray diffraction XRD (Philips X'Pert with $\text{CuK}\alpha$ radiation) technique was applied. The microstructure observations were performed using scanning electron microscope SEM (Nova Nano SEM 200 FEI & Oxford Instruments).

Results and discussion

Phase composition, structure and microstructure

Figure 1 shows the comparison of representative XRD data obtained for different groups of materials investigated in this work. Based on the XRD results [22], it can be stated that in the case of $\text{BaCeO}_{3-\delta}$ materials, the orthorhombic structure (Pmnc) changes to more symmetrical structures (tetragonal and trigonal) when the Ti is introduced into the lattice up to $x = 0.2$. In the case of Ti ($x = 0.05$)- and Y ($0 \leq y \leq 0.2$)-doped materials, the single perovskite (Pnma) phase was found for all compositions. The introduction of smaller amounts ($x = 0.01$ – 0.10) of Sn into the $\text{BaCe}_{1-x}\text{Sn}_x\text{O}_{3-\delta}$ lattice leads to the materials crystallizing in orthorhombic structure (Imma), while for higher concentrations, the trigonal (R-3c) phase was found. In the case of Sn ($x = 0.05$) and In ($0 \leq y \leq 0.2$) doped materials, only orthorhombic (Imma) structure was detected. More detailed studies concerning the influence of Sn and In

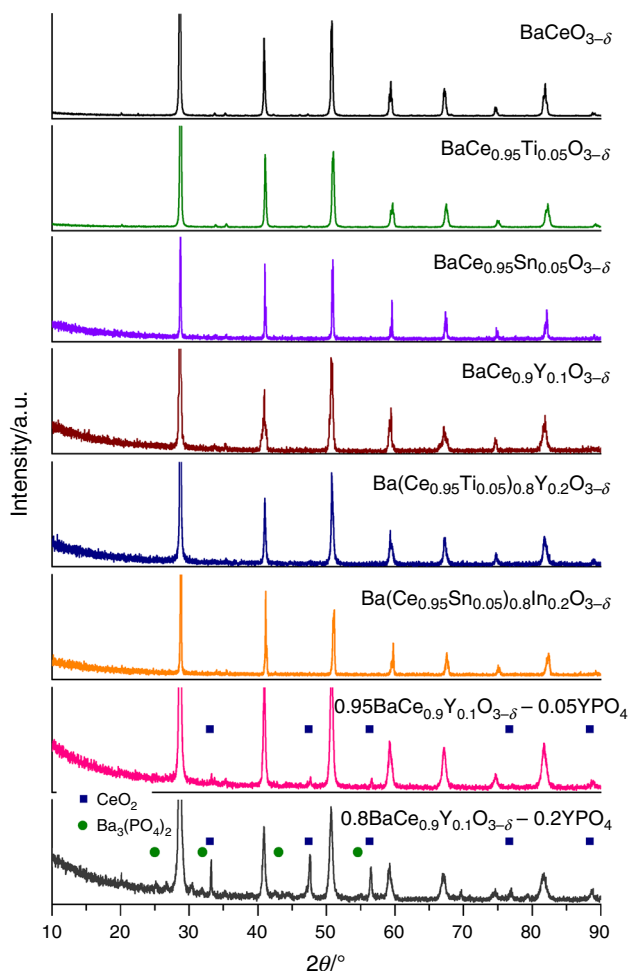


Fig. 1 XRD results of representative samples of $\text{BaCeO}_{3-\delta}$ -based materials

dopants on crystallographic structure of $\text{Ba}(\text{Ce}_{1-x}\text{Sn}_x)_{1-y}\text{In}_y\text{O}_{3-\delta}$ materials are under the way; the results will be published later.

Completely different situation is observed in the case of composite materials with the nominal formula of $(1-x)$

$\text{BaCe}_{1-y}\text{Y}_y\text{O}_{3-\delta-x}\text{Y}(\text{PO}_4)_3$. Depending on the used amount of the modifying phosphate, the $\text{BaCe}_{0.9}\text{Y}_{0.1}\text{O}_{3-\delta}$ material was obtained with possible glassy phase with undefined composition and with some traces of CeO_2 (for $x = 0.05$). In the case of higher amounts of phosphates used ($0.1 \leq x \leq 0.2$), additional $\text{Ba}_3(\text{PO}_4)_2$ phase was found, according to the reaction (8). Irrespectively of the phosphate formed (Ba or Y), the multi-phase composite material was obtained with improved chemical stability, as shown below.

Figure 2 shows the example SEM images of fractured $\text{BaCeO}_{3-\delta}$ sample. In the case of undoped $\text{BaCeO}_{3-\delta}$, the dense material with average grain size of several μm can be observed. The introduction of yttrium dopant does not lead to significant changes in microstructure, only smaller grain size can be observed. Figure 3 shows the SEM images of fractured $\text{BaCeO}_{3-\delta}$ samples modified with Ti and Sn. Introduction of Ti leads to the lower porosity comparing to the Sn dopant. In case of titanium, no dependence on Ti concentration can be observed; while in the case of tin doping, the increase of Sn concentration leads to the increase of porosity and decrease of the average grain size.

In the case of composite materials, the microstructure similar to undoped material can be observed. The smaller grains are present, caused by Y doping. Also, the grains of second phase $\text{Ba}_3(\text{PO}_4)_2$ can be recognized.

The described influence of dopants on crystallographic structure and microstructure is essential in interpretation of the chemical stability of investigated materials. Namely, the Goldschmidt tolerance factor describing the stability of the perovskite structure and the porosity will be used during discussion of chemical stability results presented below.

Chemical stability

Materials for application in electrochemical devices such as fuel cells or high-temperature membranes must exhibit stable

Fig. 2 SEM microphotograph of $\text{BaCeO}_{3-\delta}$ samples after sintering ($1,600^\circ\text{C}$, 3 h, air). Magnification $\times 5000$ (a), $\times 10000$ (b)

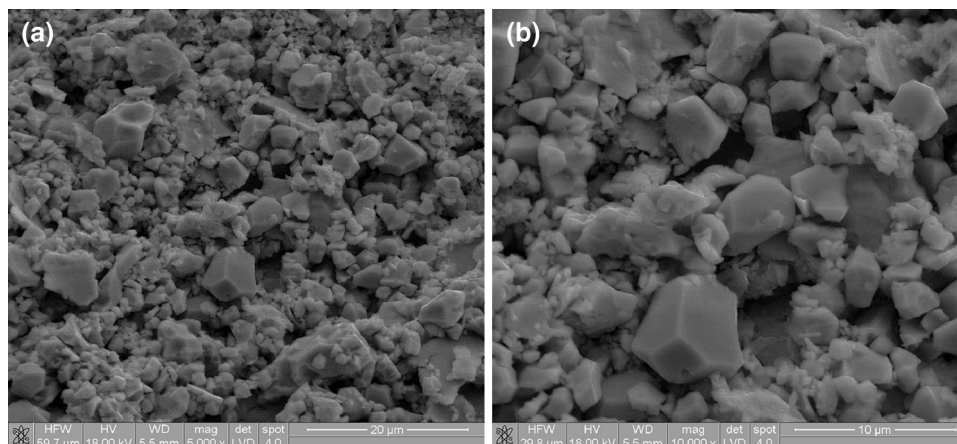
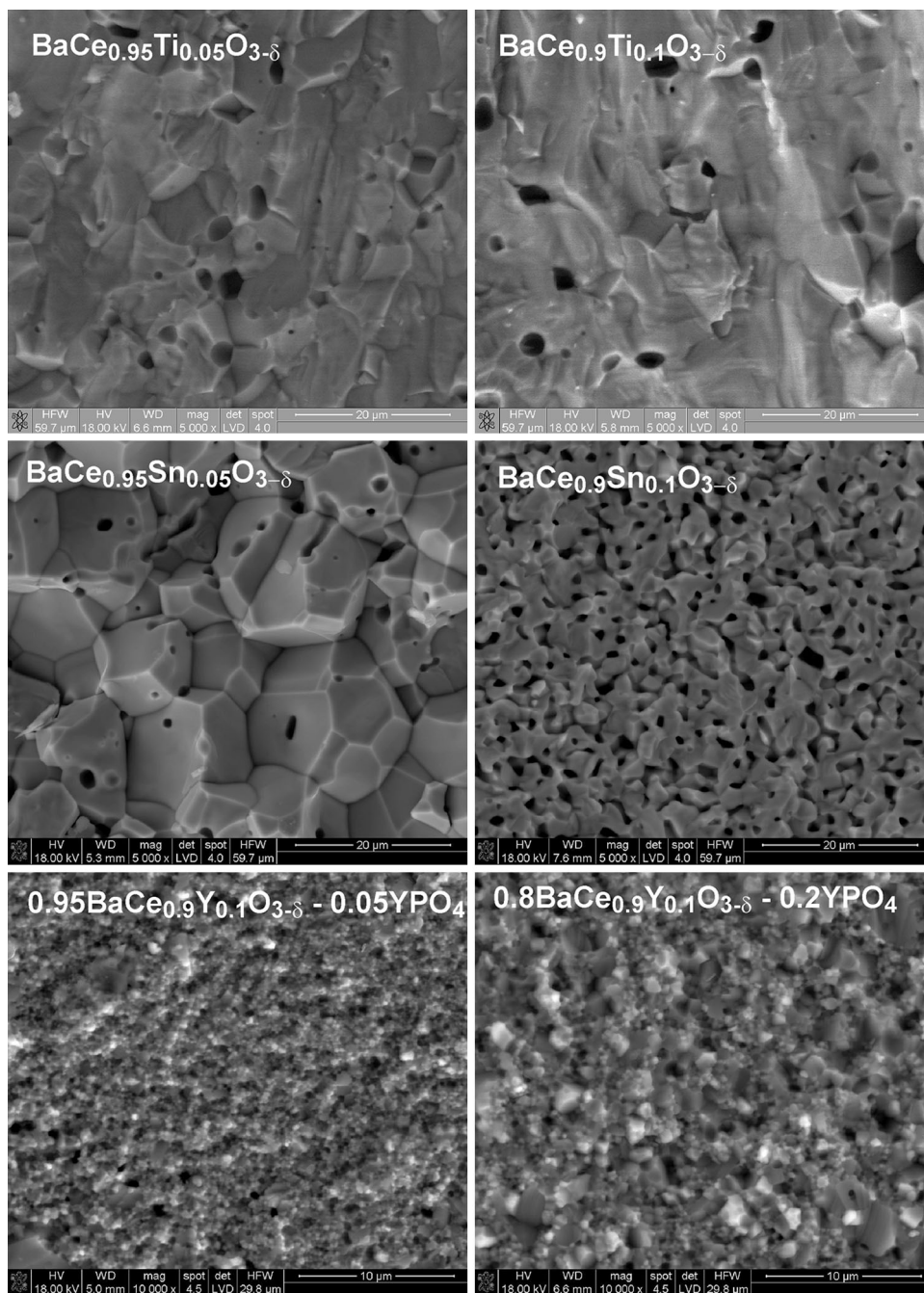


Fig. 3 SEM images of $\text{BaCeO}_{3-\delta}$ -based materials with different nominal compositions. Magnification $\times 5000$ ($\text{BaCe}_{1-x}\text{Ti}_x\text{O}_{3-\delta}$, $\text{BaCe}_{1-x}\text{Sn}_x\text{O}_{3-\delta}$); $\times 10000$ ($(1-x)\text{BaCe}_{0.9}\text{Y}_{0.1}\text{O}_{3-\delta}-x\text{YPO}_4$)

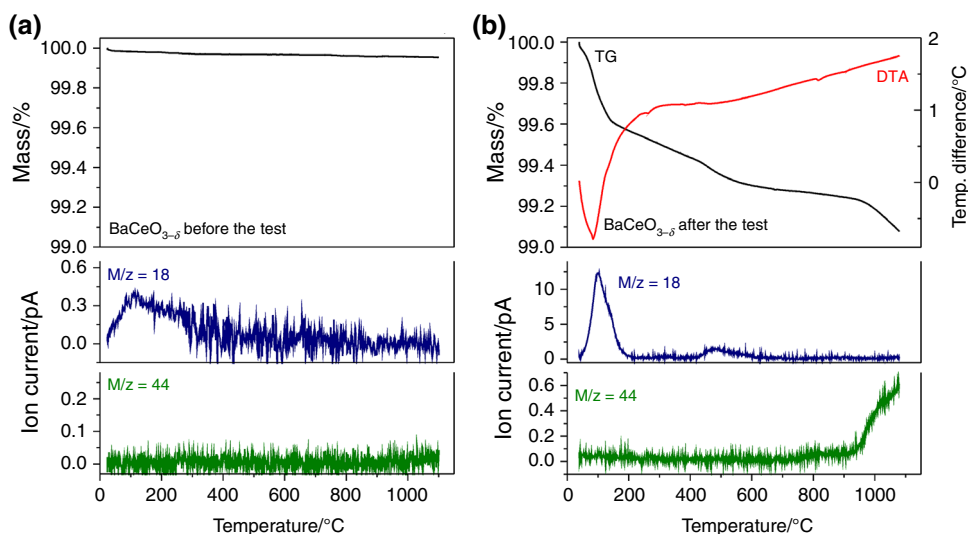


properties in atmospheres containing CO_2 , water vapour and hydrocarbons. The modifications of $\text{BaCeO}_{3-\delta}$ material by Ti, Sn, Y, In and by formation of composite materials with phosphates presented in this work were done to improve the chemical stability and increase the electrical conductivity. In order to determine quantitatively the influence of used modifications of $\text{BaCeO}_{3-\delta}$ on chemical stability in the presence of CO_2 and H_2O vapour, the comparative test based on DTA-TG coupled with MS measurements was employed. The DTA-TG-MS techniques were found to be a useful tool for such purposes [1, 8, 23].

All prepared samples under the test were exposed to the atmospheres containing CO_2 and H_2O vapour for the same period of time, to allow quantitative comparison of the dopants used on chemical stability. The amount of barium carbonate and barium hydroxide formed during the exposition can be directly determined from the mass loss observed on TG curves of the samples. Thus, this mass loss is strictly correlated with the chemical instability of the materials. The details of the test procedure are given in experimental part.

Figure 4 shows TG/MS results for $\text{BaCeO}_{3-\delta}$ before and after the exposition tests. For the material before the

Fig. 4 TG/DTA/MS results for $\text{BaCeO}_{3-\delta}$ before (a) and after (b) the exposition test



exposition, only insignificant mass loss around 0.05 % (in the temperature below 200 °C) caused by the liberation of water absorbed on the surface of material is observed (Fig. 4a). The TG curve for $\text{BaCeO}_{3-\delta}$ after the exposition test shows gradual mass loss in the entire temperature range, leading to the total mass loss of 0.9 % at 1,100 °C (Fig. 4b). The TG/DTA curves and ion current lines suggest three steps of the decomposition of secondary products formed during the exposition test. The first one, for the temperatures below 200 °C, is the release of water. The low temperature of the process suggests dehydration of material and liberation of the water absorbed on the surface and in the pores of sintered $\text{BaCeO}_{3-\delta}$. The next step in the temperature range 400–600 °C can be attributed to the decomposition of barium hydroxide $\text{Ba}(\text{OH})_2$ or destruction of protonic defects in dry air atmosphere, as reported in literature [24, 25]. According to the literature, the decomposition temperature of pure $\text{Ba}(\text{OH})_2$ is about 410 °C [24]. The last step in the temperatures above 800 °C can be described as decomposition of secondary BaCO_3 formed during the exposition test. As it is reported in the literature, the temperature of decomposition of BaCO_3 is above 900 °C however strongly depends on the decomposition atmosphere [26].

Figure 5 shows the representative TG results for $\text{BaCe}_{0.9}\text{Y}_{0.1}\text{O}_{3-\delta}$, $\text{BaCe}_{0.95}\text{Ti}_{0.05}\text{O}_{3-\delta}$, $\text{Ba}(\text{Ce}_{0.95}\text{Ti}_{0.05})_{0.8}\text{Y}_{0.2}\text{O}_{3-\delta}$, $\text{BaCe}_{0.95}\text{Sn}_{0.05}\text{O}_{3-\delta}$, $\text{Ba}(\text{Ce}_{0.95}\text{Sn}_{0.05})_{0.8}\text{In}_{0.2}\text{O}_{3-\delta}$ and composite material with nominal composition $0.95\text{BaCe}_{0.9}\text{Y}_{0.1}\text{O}_{3-\delta}-0.05\text{YPO}_4$ before the exposition test. Figure 6 shows TG results for the samples with the same compositions, but after the exposition test. Analogical measurements were performed for all prepared samples.

According to the data presented in Fig. 5, the mass loss of all materials before the exposition test is very low, below 0.35 %. It indicates that as-prepared samples, stored

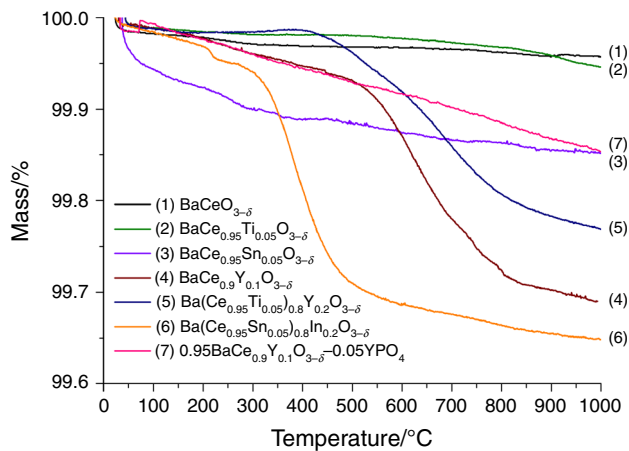


Fig. 5 TG curves of representative sinter samples of $\text{BaCeO}_{3-\delta}$ -based materials before exposition test

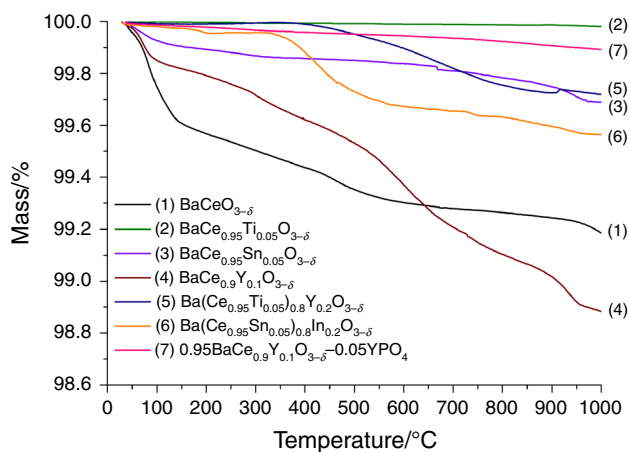


Fig. 6 TG curves of representative sinter samples of $\text{BaCeO}_{3-\delta}$ -based materials after exposition test (7 % of CO_2 in air, 100 % RH, 350 h, 25 °C)

in desiccator before the exposition test, are almost free from any secondary barium carbonate or hydroxide. In the case of acceptor-doped samples (samples 4, 5, 6), the mass loss is caused mostly by the liberation of water molecules in the temperature range 400–600 (750) °C, which can be attributed to the destruction of protonic defects. Acceptor-doped materials exhibit much higher concentration of such defects than undoped materials, according to the Eq. (3) describing the formation of protonic defects. The rest of the samples exhibit smaller mass loss, not >0.15 %.

After the exposition test, samples are divided into two apparent groups, as shown in Fig. 6. The reference samples $\text{BaCeO}_{3-\delta}$ and $\text{BaCe}_{0.9}\text{Y}_{0.1}\text{O}_{3-\delta}$ exhibit noticeable higher mass loss (0.8–1.2 %) comparing to the modified samples (by Ti or Sn or composite) where the total mass loss is not higher than 0.4 %. Again, acceptor-doped sample ($\text{BaCe}_{0.9}\text{Y}_{0.1}\text{O}_{3-\delta}$) shows higher mass loss, comparing to undoped one ($\text{BaCeO}_{3-\delta}$), especially at higher temperatures. Presented results indicate that doping by isovalent dopant (Ti, Sn) leads to the improvement of chemical stability, especially in the presence of CO_2 . It is in agreement with the results reported previously [8, 27, 28], where the correlation between the crystallographic structure (symmetry) and chemical stability was shown.

In case of composite materials, the improvement of chemical stability can be also noticed. In this case, the modification of grain boundaries by the presence of the additional phase may be postulated, thus blocking the possible ways of deterioration process.

The detailed discussion of presented results may be extended based on the analysis of Goldschmidt tolerance factor, S , describing the departure from ideal cubic perovskite structure [28]:

$$S = \frac{r_A + r_O}{\sqrt{2}(r_B + r_O)}$$

where r_A , r_B and r_O describe the ionic radii of A, B and O ions in ABO_3 perovskite structure, respectively.

According to the literature data [27, 28], generally the higher Goldschmidt tolerance factor, the better chemical stability of material is expected. In order to discuss the influence of used dopants on the chemical stability, the Goldschmidt tolerance factors were calculated using the ionic radii (Table 1), taking into calculations the weighted averages of host and guest ion radius [21, 29].

Figure 7 shows the dependence of measured mass loss on the calculated Goldschmidt tolerance factors for all investigated samples. Taking into account that mass loss can be treated directly as a measure of chemical instability and the Goldschmidt tolerance factor describes the crystallographic structure, the influence of used modifications can be easily discussed. As can be seen, in the case of Ti-doped materials (Fig. 7a), the expected improvement of

Table 1 Ionic radii of ions used to calculate Goldschmidt tolerance factors for $\text{BaCeO}_{3-\delta}$ -based materials [21, 29]

Ion	Coordination number	Ionic radii/nm
Ba^{2+}	12	0.160
Ce^{4+}	6	0.087
Y^{3+}	6	0.090
Ti^{4+}	6	0.061
In^{3+}	6	0.080
Sn^{4+}	6	0.069
O^{2-}	6	0.140

chemical stability was achieved by Ti doping, comparing to undoped material. Surprisingly, the higher concentration of Ti the worse stability of material was found. Such unexpected inverse dependence of mass loss versus Goldschmidt tolerance factor, S , cannot be directly clarified. The possible explanation should probably involve the influence of Ti concentration on the grain boundary properties.

In the case of yttrium-doped $\text{BaCeO}_{3-\delta}$ (for 5 % Ti), the observed dependence of mass loss versus S is as expected, the higher concentration of yttrium, the lower S and the higher mass loss (worse stability), as shown in Fig. 7b. Only for the highest concentration of Y tested (20 %), the unexpected higher stability was observed. The possible explanation can involve the yttrium content higher than solubility limit reported in the literature (10 % of yttrium in $\text{BaCeO}_{3-\delta}$) [25].

Doping by tin leads to the improvement of chemical stability, the higher concentration of tin the lower mass loss is observed, as expected (Fig. 7c). Taking into account the influence of tin concentration on microstructure, as shown in Fig. 3, it can be stated that the modification of microstructure by tin does not affect the chemical stability.

In the case of doping by indium (for 5 % of Sn), the observed dependence of mass loss on Goldschmidt tolerance factor is in disagreement with expected one; the higher S , the worse chemical stability (Fig. 7d). This observation can be explained taking into account higher concentration of oxygen vacancies formed according to the reaction (3) due to increasing concentration of acceptor dopant. Thus, the mechanism of formation of secondary barium carbonate must involve the role of oxygen vacancies and higher diffusivities of ions in acceptor-doped materials comparing to undoped one. The role of structure symmetry has the minor impact in such cases.

Generally, based on the presented results concerning chemical stability of $\text{BaCeO}_{3-\delta}$ -based materials, it can be stated that the analysis of the influence of different dopants on structure symmetry described by Goldschmidt tolerance factor is not sufficient. The role of defect chemistry modification, the role of grain boundaries and microstructure

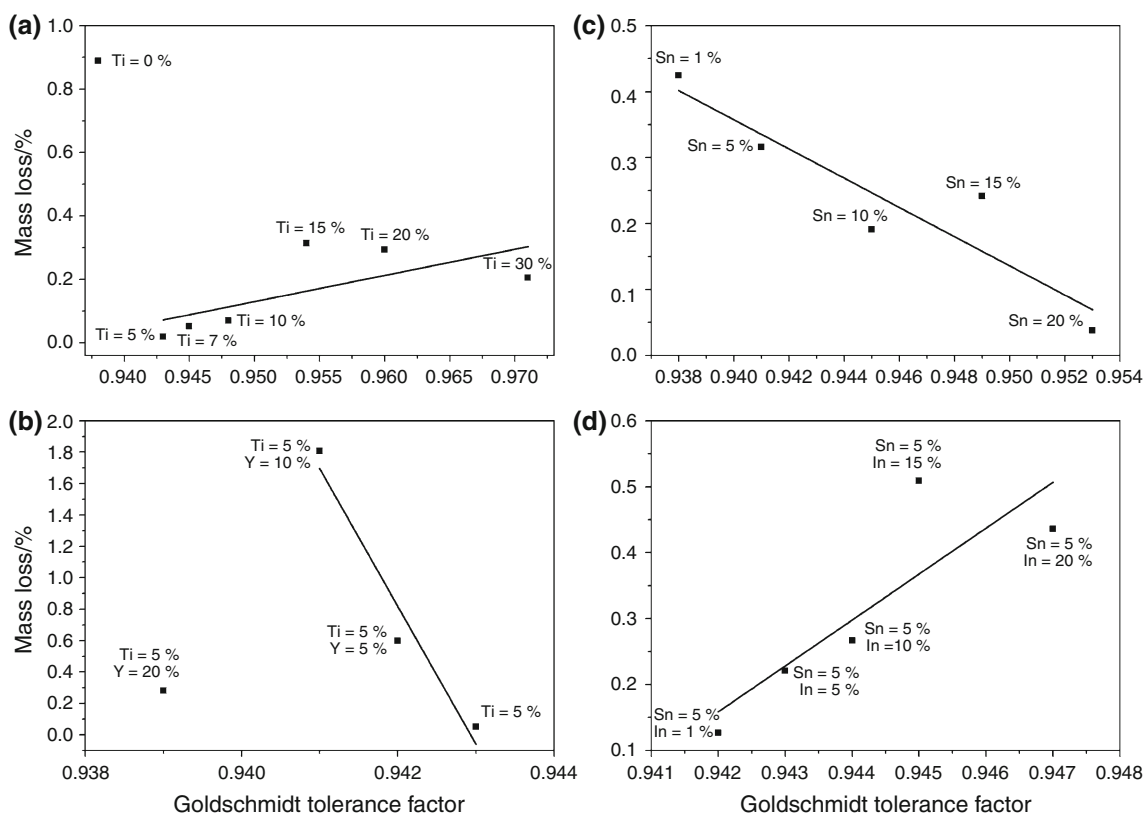


Fig. 7 Mass loss after the exposition test as a function of Goldschmidt tolerance factor calculated for $\text{BaCe}_{1-x}\text{Ti}_x\text{O}_{3-\delta}$ ($x = 0.05\text{--}0.3$) (a), $\text{Ba}(\text{Ce}_{1-x}\text{Ti}_x)\text{Y}_y\text{O}_{3-\delta}$ ($x = 0.05$, $y = 0.05\text{--}0.2$) (b), $\text{BaCe}_{1-x}\text{Sn}_x\text{O}_{3-\delta}$

($x = 0.01\text{--}0.2$) (c) and $\text{Ba}(\text{Ce}_{1-x}\text{Sn}_x)\text{In}_y\text{O}_{3-\delta}$ ($x = 0.05$, $y = 0.01\text{--}0.2$) (d) samples

must be taken into account, especially in the cases when the changes of Goldschmidt tolerance factor caused by doping are relatively low.

Conclusions

In this work, the results concerning the chemical stability of barium cerium oxide-based materials tested using DTA and TG techniques were presented. Also, the structural and microstructural properties of these materials were studied, in order to assist the interpretation of chemical stability results.

Different groups of materials based on $\text{BaCeO}_{3-\delta}$ were synthesized and investigated. The phase composition, crystallographic structure, microstructure, and the chemical stability in the presence of CO_2 and H_2O , were determined as a function of chemical composition of synthesized materials. The correlation of chemical stability on Goldschmidt tolerance factor, describing the deviation from ideal perovskite structure, was found in most of the materials investigated. Additionally, the role of defect chemistry modification and microstructure must be taken into account when explaining the influence of used modifications on chemical stability of materials.

It was found that DTA-TG technique is the especially an useful tool to compare the chemical stability of different materials. The mass loss can be treated directly as a measure of chemical instability of materials under the condition that all materials were exposed to the same corroding conditions (the same gas atmosphere and time). The corrosion tests conditions applied in this work (350 h at room temperature in CO_2 7 % and H_2O 100 % RH) were found to be well optimized for the group of materials tested. Namely, the mass loss was high enough to be measured using the TG technique, from the other hand, the secondary corrosion reaction was not complete (not the whole material was converted into secondary carbonates or hydroxides), thus the saturation of signal was not observed.

The DTA-TG technique was found useful for our test not only from the point of view of determination of mass loss as a direct measure of chemical instability, but also from the point view of interpretation of corrosion mechanism. Each mass loss clearly seen on TG curve correlated with the endothermic effects of DTA curve can be assigned, depending on the temperate, to the dehydration of the materials, decomposition of the secondary formed $\text{Ba}(\text{OH})_2$, destruction of protonic defects or finally the decomposition of BaCO_3 formed as the result of chemical instability of barium cerate.

Obtained results can be also useful for determination of the optimal composition of intermediate temperature ceramic protonic conductor suitable for potential future applications.

Acknowledgements The financial support of Polish National Science Centre (NCN), Project No. DEC 2011/01/B/ST5/06427 (AGH No. 18.18.160.189) is acknowledged.

Open Access This article is distributed under the terms of the Creative Commons Attribution License which permits any use, distribution, and reproduction in any medium, provided the original author(s) and the source are credited.

References

- Ryu KH, Haile SM. Chemical stability and proton conductivity of doped $\text{BaCeO}_3\text{-BaZrO}_3$ solid solutions. *Solid State Ion.* 1999;125:355–67.
- Ma G, Shimura T, Iwahara H. Ionic conduction and nonstoichiometry in $\text{Ba}_x\text{Ce}_{0.90}\text{Y}_{0.10}\text{O}_{3-\delta}$. *Solid State Ion.* 1998;110:103–10.
- Katahira K, Kohchi Y, Shimura T, Iwahara H. Protonic conduction in Zr-substituted BaCeO_3 . *Solid State Ion.* 2000;138:91–8.
- Xie K, Yan R, Chen X, Dong D, Wang S, Liu X, Meng G. A new stable BaCeO_3 -based proton conductor for intermediate-temperature solid oxide fuel cells. *J Alloy Compd.* 2009;472:551–5.
- Kim J-H, Kang Y-M, Byun M-S, Hwang K-T. Study on the chemical stability of Y-doped $\text{BaCeO}_{3-\delta}$ and $\text{BaZrO}_{3-\delta}$ films deposited by aerosol deposition. *Thin Solid Films.* 2011;520:1015–21.
- Okiba T, Fujishiro F, Hashimoto T. Evaluation of kinetic stability against CO_2 and conducting property of $\text{BaCe}_{0.9-x}\text{Zr}_x\text{Y}_{0.1}\text{O}_{3-\delta}$. *J Therm Anal Calorim.* 2013;113:1269–74.
- Talimi M, Thangadurai V. Electrical conductivity and chemical stability of perovskite-type $\text{BaCe}_{0.8-x}\text{Ti}_x\text{Y}_{0.2}\text{O}_{3-\delta}$. *Ionics.* 2011;17:195–200.
- Pasierb P, Drozd-Ciesla E, Gajerski R, Labus S, Komornicki S, Rekas M. Chemical stability of $\text{Ba}(\text{Ce}_{1-x}\text{Ti}_x)_{1-y}\text{Y}_y\text{O}_3$ proton-conducting solid electrolytes. *J Therm Anal Calorim.* 2009;96:475–80.
- Azad AK, Irvine JTS. Synthesis, chemical stability and proton conductivity of the perovskites $\text{Ba}(\text{Ce}, \text{Zr})_{1-x}\text{Sc}_x\text{O}_{3-\delta}$. *Solid State Ion.* 2007;178:635–40.
- Zhong Z. Stability and conductivity study of the $\text{BaCe}_{0.9-x}\text{Zr}_x\text{Y}_{0.1}\text{O}_{2.95}$ systems. *Solid State Ion.* 2007;178:213–20.
- Takeuchi K, Loong CK, Richardson JW Jr, Guan J, Dorris SE, Balachandran U. The crystal structures and phase transitions in Y-doped BaCeO_3 : their dependence on Y concentration and hydrogen doping. *Solid State Ion.* 2000;138:63–77.
- Oishi M, Akoshima S, Yashiro K, Sato K, Mizusaki J, Kawada T. Defect structure analysis of B-site doped perovskite-type proton conducting oxide BaCeO_3 Part 1: the defect concentration of $\text{BaCe}_{0.9}\text{M}_{0.1}\text{O}_{3-\delta}$ ($\text{M} = \text{Y}$ and Yb). *Solid State Ion.* 2009;180:127–31.
- Chen FL, Sørensen OT, Meng GY, Peng DK. Preparation of Nd-doped BaCeO_3 proton-conducting ceramic and its electrical properties in different atmospheres. *J Eur Ceram Soc.* 1998;18:1389–95.
- Vaquero-Aguilar C, Jiménez-Melendo M. Characterization and creep properties of proton-conducting Yb-doped barium cerate. *J Eur Ceram Soc.* 2011;31:2671–6.
- Pornprasertsuk R, Yuwattanawong C, Permkittikul S, Tungtidtham T. Preparation of doped BaZrO_3 and BaCeO_3 from nanopowders. *Int J Precis Eng Man.* 2012;13:1813–9.
- Sawant P, Varma S, Wani BN, Bharadwaj SR. Influence of synthesis route on morphology and conduction behavior of $\text{BaCe}_{0.8}\text{Y}_{0.2}\text{O}_{3-\delta}$. *J Therm Anal Calorim.* 2012;107:189–95.
- Guo Y, Lin Y, Ran R, Shao Z. Zirconium doping effect on the performance of proton-conducting $\text{BaZr}_y\text{Ce}_{0.8-y}\text{Y}_{0.2}\text{O}_{3-\delta}$ ($0.0 \leq y \leq 0.8$) for fuel cell applications. *J Power Sources.* 2009;193:400–7.
- Medvedev DA, Gorbova EV, Demin AK, Antonov BD. Structure and electric properties of $\text{BaCe}_{0.77-x}\text{Zr}_x\text{Gd}_{0.2}\text{Cu}_{0.03}\text{O}_{3-\delta}$. *Russ J Electrochem.* 2011;47:1404–10.
- Talimi M, Thangadurai V. Electrical conductivity and chemical stability of perovskite-type $\text{BaCe}_{0.8-x}\text{Ti}_x\text{Y}_{0.2}\text{O}_{3-\delta}$. *Ionics.* 2011;17:195–200.
- Robinson S, Manerbino A, Coors WG, Sullivan NP. Fabrication and performance of tubular, electrode-supported $\text{BaCe}_{0.2}\text{Zr}_{0.7}\text{Y}_{0.1}\text{O}_{3-\delta}$ fuel cells. *Fuel Cells.* 2013;13:584–91.
- Shannon RD. Revised effective ionic radii and systematic studies of interatomic distances in halides and chalcogenides. *Acta Crystallogr.* 1976;A32:751–67.
- Pasierb P, Drozd-Ciesla E, Rekas M. Properties of $\text{BaCe}_{1-x}\text{Ti}_x\text{O}_3$ materials for hydrogen electrochemical separators. *J Power Sources.* 2008;181:17–23.
- Łącz A, Pasierb P. Synthesis and properties of $\text{BaCe}_{1-x}\text{Y}_x\text{O}_{3-\delta}$ - BaWO_4 composite protonic conductors. *J Therm Anal Calorim.* 2013;113:405–12.
- Habashy GM, Kolta GA. Thermal decomposition of the hydrates of barium hydroxide. *J Inorg Nucl Chem.* 1972;34:57–67.
- Pasierb P. Properties of BaCeO_3 protonic conductors modified by Ti and Y. *Ann Chim-Sci Mat.* 2008;33:157–64.
- Galwey AK, Brown ME. Thermal decomposition of ionic solids. Amsterdam: Amsterdam Elsevier Science B.V.; 1999.
- Haile SM, Staneff G, Ryu KH. Non-stoichiometry, grain boundary transport and chemical stability of proton conducting perovskites. *J Mater Sci.* 2001;36:1149–60.
- Takayama-Muromachi E, Navrotsky A. Energetics of compounds ($\text{A}^{2+}\text{B}^{4+}\text{O}_3$) with the perovskite structure. *J Solid State Chem.* 1988;72:244–56.
- Jia YQ. Crystal radii and effective ionic radii of the rare earth ions. *J Solid State Chem.* 1991;95:184–7.